IEEE Access
Multidisciplinary | Rapid Review | Open Access Journal

Received January 3, 2022, accepted January 20, 2022, date of publication January 25, 2022, date of current version March 3, 2022.

Digital Object Identifier 10.1109/ACCESS.2022.3145974

Transient Electromagnetic Weak Signal Extraction Method Based on Multi-Scale Combined Difference Product Morphological Filtering

JIANSHENG BAI, JINJIE YAO, ZHILIANG YANG, YURONG GUO, AND LIMING WANG
State Key Laboratory for Electronic Testing Technology, North University of China, Taiyuan 030051, China
School of Information and Communication Engineering, North University of China, Taiyuan 030051, China

Corresponding author: Liming Wang (wlm@nuc.edu.cn)

This work was supported in part by the Research on Wireless Intrusion Monitoring System for Critical Information Infrastructure, in part by the Key Research and Development Plan of Shanxi Province (high-tech field) under Grant 201903D111002, and in part by the Shanxi Province Graduate Student Innovation Project under Grant 2021Y607.

ABSTRACT To solve the problem of poor recognition effect of transient signal in low Signal-to-Noise ratio (SNR) and strong interference electromagnetic environment, a morphological filtering method based on the multi-scale combined difference product (MCDPMF) was proposed. This paper concentrates on the issues of sudden changes in transient electronic signal, such as impulses and edges. Firstly, it provides a difference product morphological filter. Moreover, the extended and multi-origin morphological Structural Elements (*SEs*) is constructed, combining with the multi-structural layers $\boldsymbol{a}$ ($\boldsymbol{a}$ indicates the structural layers of the MCDPMF), the transient electromagnetic weak signal is multi-scale filtered. They are used to optimize the number of the structure layers $\boldsymbol{a}$ adaptively based on the amplitude characteristic ratio of the positive and negative polarity of the filtered signal (HML value), combining the kurtosis-SNR ($k_x - SNR$) ratio characteristic coefficient. MCDPMF is proposed to enhance the filtering results and suppress the noise frequency points. Meanwhile, it can extract the structure components and identify the features of the transient electromagnetic weak signal. It can be shown from simulation and experimental results that the proposed method is superior to EMD, AVG, OCCO, and other methods in subjective evaluation and objective indicators.

INDEX TERMS Transient electromagnetic signal, weak signal extraction, morphological filtering, multi-scale combined difference.

I. INTRODUCTION

With the development of wireless communication, the communication signal system and modulation style are becoming more complex and more diverse. The frequency spectrum is developing increasingly crowded and overlapped, leading to a significant increase in background noise and interference [1]. The extraction of weak transient electromagnetic signals can analyze the coupling characteristics of electromagnetic interference signals. Meanwhile, electromagnetic signals also contain a large amount of character information that can characterize the interference intensity of electromagnetic emission sources and the types of abnormal signals. Transient electromagnetic signals have non-stationary characteristics typically. They appear as single or multiple periodic pulse signals in the time domain with sharp changes in amplitude, extremely fast rising and falling edges, as well as extremely short duration. At the same time, the frequency of interfering sources is complicated, and the components are unpredictable [2], leading to the pulse signal being submerged by strong background noise and interfering components. Therefore, it is challenging to extract and identify the structure of weak electromagnetic transient signals under strong background noise.

There are many electromagnetic signal detection methods under strong background noise, all of which have achieved good extraction results, such as mechanical fault signal diagnosis, weak vibration signal extraction, etc [3], [4]. In traditional transient signal detection methods, the short-time spectral correlation method requires prior knowledge

The associate editor coordinating the review of this manuscript and approving it for publication was Baoping Cai.

of the detected signal [5], [6]. Power-Law detection method [7], transient energy detection method [8], and cepstral analysis [9] results are greatly affected by noise. Besides, the detection performance deteriorates sharply or even fails in a low SNR environment. In time-frequency analysis methods, Hilbert-Huang transform [10], Empirical mode decomposition (EMD) [11], learning modulation filter network (LMFN) [12], and Convolutional Neural Network [13], [14] are introduced to preprocess transient signals. However, in essence, the transient energy is used as the measurement, which increases the amount of calculation in the process of signal extraction, and its applicability is poor.

Morphological filter [15], [16] is a nonlinear filtering processing method [17] based on mathematical morphological transformation. Morphological filtering is widely used in image processing [18], speech recognition, fault diagnosis, and other fields [19], [20]. In recent years, it has been applied in detecting transient signals and achieved good application effects [21], [22], especially in expanding morphological operators' construction, the optimal *SE* selection and adaptive morphological filter [23], which has become a research hotspot [24]–[27]. The morphological filter combined with the structural element (*SE*) as the filtering window [28] to matche the geometric features of the signal to be analyzed. It modifies the local signals in the time domain [29], [30], effectively extracting the signal's edge contour and shape features. Morphological filtering can effectively remove large-scale noise interference and baseline drift that are aliased in the signal. It can identify, reconstruct, and enhance the potential morphology for distorted signals. However, the morphological filtering method for transient signal extraction has two problems: (1) Strong background noise environment's interference components are complex. The traditional morphological filters have simple structures, such as Differentiation gradient (MG) [31] and Mathematical morphology (MM) [32], which are prone to produce truncation errors when removing interfering harmonic signals. The useful electromagnetic signal is still retained in the separated noise signal, and thus detection errors arise [33]. EDMF [19], DIF (Difference Filter) [34], ACDIF [35] combined with classical morphological operators can alleviate detection error, and has been applied to the device's fault transient signal reduction. However, these methods cannot evaluate different SNR ratios' detection effects effectively. They aren't universal for they only focus on the results of frequency filtering of transient signal, but little on the characteristics of the signal structure. (2) In proposing morphological filters, the construction of morphological operators and the selection of *SE* are mainly considered. For example, the Kurtosis criteria (KR) [36] and Feature energy factor (FEF) [37] are used to select the optimal *SE* scale and shape. Combining with traditional morphological operators to construct new operators AVG (Average operator) [29], OCCO [38] to enhance the extraction of weak signals, but the role of structural layers $\boldsymbol{a}$ [39] in morphological filtering is ignored.

To solve the above problems, this article proposes a multi-scale combined difference product morphological filtering method (MCDPMF). The main contributions are as follows: With the breakthrough of strong noise and abnormal frequency point suppression based on the morphological filtering, the filtering effect under different SNR ratio is discussed by using the extensible, multi-origin, and multi-scale SEs and the multi-structural layers $\boldsymbol{a}$ optimized by characteristic parameter index. A multi-scale combined difference product morphological filter is constructed to enhance the filtering results. Finally, the structure and feature extraction of transient weak signals in a strong noise electromagnetic environment is realized. The method proposed in this paper is feasible and superior in extracting transient electromagnetic weak signals under strong background noise, based on simulation and experimental results.

II. BASIC OPERATION IN MATHEMATICAL MORPHOLOGY

In mathematical morphology, expansion and corrosion operations constitute a pair of dual transformations. The corrosion operator has the function of weakening the peak and strengthening the trough of the signal. The expansion operator can weaken the trough and strengthen the peak. At the same time, the open operation can suppress the positive pulse of the signal and extract the negative pulse, as well as the closed operation is the opposite [27], [40]. Combined with the filtering characteristics of the four basic morphological operators, it can form a better operator to extract the characteristic information of electromagnetic transient weak signal from strong background noise. In addition to ensuring that the shape of the transient electromagnetic signal is not damaged, the closed operation and expansion operation are calculated to enhance the retention of positive pulses and the suppression of negative pulses. And then, the negative pulse retained in the transient signal is corrected through the cascade of corrosion operation. The constructed operators F_{CDE} and F_{DCE} are defined as follows [18]:

$$F_{CDE}(f) = f \cdot g^{+} \oplus g^{+} \tag{1}$$

$$F_{DCE}(f) = f \oplus g^{+} \cdot g^{+} \tag{2}$$

Similarly, the open operation and corrosion operation are cascaded to enhance the retention of negative pulses and the suppression of positive pulses. Then the retained positive pulses in the transient signal are modified through the cascade of expansion operation. The constructed operators F_{EOD} and F_{OED} are defined as follows:

$$F_{EOD}(f) = f \Theta g^{-} \circ g^{-} \tag{3}$$

$$F_{OED}(f) = f \circ g^{-} \Theta g^{-} \tag{4}$$

In Eq. (1)-(4), g^{+} and g^{-} are represent *SEs*, which slide in the signal like a mobile filtering window to check its interaction and extract specific features.

III. MULTI-SCALE COMBINED DIFFERENCE PRODUCT MORPHOLOGICAL FILTERING METHOD

A. DEFINITION OF MCDPMF

The *SEs* constructed in this paper are as follows:

$$\begin{aligned} g^{+} &= \min A_a\{g_1, g_2, \cdots g_{l-1}, \underline{g_l}\} \\ g^{-} &= -\min A_a\{\underline{g_1}, g_2, \cdots g_{l-1}, g_l\} \end{aligned} \tag{5}$$

In Eq. (5), g^+ and g^- are used to extract the rising and falling edge of the transient electromagnetic signal respectively. $minA_a$ represents the minimum amplitude of the signal when the number of structural layers is $\boldsymbol{a}$, l represents the length of *SEs*, and satisfies this equation $l = 2^{l-a}lg$ [15]. l_g is the length of $\boldsymbol{a}$ when g is equal to 1. The underlined samples in g^+ and g^- indicate the origin of the g.

In order to enhance the ability to extract transient electromagnetic signals under strong noise, based on the filtering characteristics of operators, such as the F_{CDE}, F_{DCE}, F_{EOD} and F_{OED}, a combined difference product morphological filter (CDPMF) is proposed firstly, which uses the form of combined difference products of four types of operators to compensate performance deficiencies of various operators and achieve effective extraction of weak signals. When the number of structural layers is a, the definition of P_g^a is as follows:

$$\begin{aligned} P_{g+}^a &= (F_{CDE}^a - F_{EOD}^a)(x) \times (F_{DCE}^a - F_{OED}^a)(x) \\ P_{g-}^a &= -(F_{EOD}^a - F_{CDE}^a)(x) \times (F_{OED}^a - F_{DCE}^a)(x) \end{aligned} \tag{6}$$

In Eq. (6), P^0 represents the original signal. Since $F_{CDE}|F_{DCE} \geq F_{EOD}|F_{OED}$, so $P_{g^+}^a \geq 0$ and $P_{g^-}^a \leq 0$. $P_{g^+}^a$ and $P_{g^-}^a$ correspond to the rising edge and falling edge of the signal respectively, namely the polarity of the transient signals. The definition of CDPMF is as follows:

$$\begin{aligned} CDPMF = &\left[(F_{CDE} - F_{OED})/2 \cdot (F_{DCE} - F_{EOD})/2\right](f) \\ &- \left[(F_{EOD} - F_{CDE})/2 \cdot (F_{OED} - F_{DCE})/2\right](f) \end{aligned} \tag{7}$$

In combination with Eq. (6), Eq. (7) can be written as:

$$CDPMF = \left[P_{g+}^a/4\right](f) + \left[P_{g-}^a/4\right](f) \tag{8}$$

In this paper, multi-structure layers are used to perform morphological operations on signals, combined with Eq. (8) to construct a multi-scale combined difference product morphological filter (MCDPMF), which is defined as follows:

$$MCDPMF = \begin{cases} \left[P_{g+}^{a_1}/4\right](f) + \left[P_{g-}^{a_1}/4\right](f) = f_1 \\ \left[P_{g+}^{a_2}/4\right](f_1) + \left[P_{g-}^{a_2}/4\right](f_1) = f_2 \\ \vdots \\ \left[P_{g+}^{a_i}/4\right](f_{i-1}) + \left[P_{g-}^{a_i}/4\right](f_{i-1}) = f_i \end{cases} \tag{9}$$

where f is the original transient electromagnetic signal, $f_1 \cdots f_i$ is the signal filtering effect under different $\boldsymbol{a}$, $a_1 \cdots a_i$ is the number of layers in different structures, $P_g^{a1} \cdots P_g^{ai}$ is the combined difference product morphological operator under different resolutions. The MCDPMF filter constructed in this paper can effectively take the anti-noise performance and the ability to maintain the details of the electromagnetic signal into account, overcoming the limitation of the filtering ability of a single morphological filter operator. It can also suppress the steady-state component of the target signal, enhance the transient component, and realize the suppression of abnormal frequency points and signal extraction of electromagnetic signals in a strong noise environment.

B. SELECTION PRINCIPLE OF SEs OPERATOR

Transient electromagnetic weak signal has complex frequency components and high steepness, and the weak pulse characteristics under strong noise make it highly nonlinear. This article combines Eq. (5) to design scalable, multi-origin, multi-scale *SEs* to analyze the signal. Transient signals in small-scale *SEs* can better extract details and retain steep transient non-stationary high-frequency signals in low SNR environments. Large-scale *SEs* can better filter out interference and noise and obtain the contour characteristics of the signal, which makes up for the denoising ability of small-scale *SEs* [37]. Combined with signal characteristics, a new operator of the sinusoidal structure element is designed in this paper. The shape of the operator is shown in Fig.1:

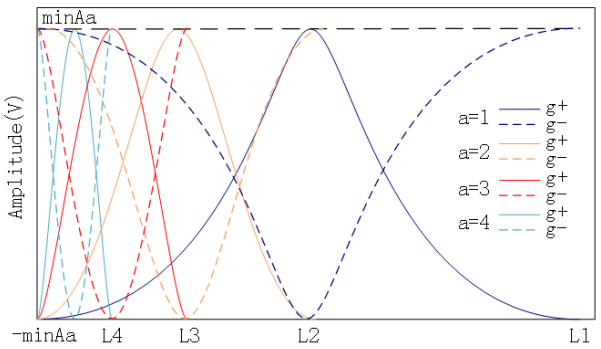

FIGURE 1. The SEs operator designed in this paper.

As shown in Fig.1, L is the length of *SEs*, and $minA_a$ is the lowest amplitude of the positive pulse of the transient electromagnetic signal when the number of structural layers is $\boldsymbol{a}$. $-minA_a$ is the lowest amplitude of the negative pulse of the signal. The *SEs* operator constructed in this paper has the same shape and amplitude under different conditions of $\boldsymbol{a}$, but the difference is the length. With the increase of $\boldsymbol{a}$, the processing window of each layer of structural element operator decreases, and the distinction of signal characteristics will be more obvious.

C. SELECTION PRINCIPLE OF STRUCTURAL LAYERS IN MCDPMF

In this paper, kurtosis's strong anti-interference ability in characterizing transient pulse signals and remarkable advantage [37], combined with SNR to form characteristic coefficients ($k_x - SNR$) to optimize the number of structural

layers $\boldsymbol{a}$. k_x indicates the peak value of the probability density distribution of the signal at the mean value. Assuming that the sampled value of the signal is n, its kurtosis can be expressed as:

$$k_x = \frac{\frac{1}{n}\sum_{i=1}^{n}(x_i - \bar{x})^4}{(\frac{1}{n}\sum_{i=1}^{n}(x_i - \bar{x})^2)^2} - 3 \tag{10}$$

where x_i represents the i_{th} value of the sampled signal and x is the average value of the sampled signal. If k_x is positive, it means that the sampled signal has a super-Gaussian distribution, with a clear upward or downward trend, and means it is a spike signal. If k_x is negative, it means that the sampling signal distribution is relatively gentle. That is to say, it is a sub-Gaussian distribution, and there is no spike or impulse.

Calculate the root mean square (RMS) of the electromagnetic signal, expressed as:

$$V_{rms} = \sqrt{\frac{1}{\tau}\int_{t_0}^{t_0+\tau} V^2(t)\,dt} \tag{11}$$

In Eq. (11), τ is the average sampling time. Signals with different SNR are set through the RMS value of the original signal $s(n)$ and noise signal $x(n)$. The mixed signal is $x(n) = s(n) + g\_noise(n)$, and the SNR value is expressed as:

$$SNR\,[dB] = 20\lg\frac{x(n)_{rms}}{s(n)_{rms}} \tag{12}$$

The random simulation was conducted for $x(n)$ and $g\_noise(n)$ for 10 times, in order to obtain the change of $k_x - SNR$ (−10dB-30dB) within $\boldsymbol{a}$ in the range of 1-6, as shown in Fig.2-Fig.3:

As Fig.2-Fig.3 shows, when SNR ranges from 10dB to 30dB, the kurtosis eigenvalues of $x(n)$ and $g\_noise(n)$ are highly distinguished, but as SNR decreases, the kurtosis eigenvalues of $x(n)$ gradually approach to $g\_noise(n)$. The $k_x - SNR$ of the simulated mixed noise signal has good stability; the maximum value is 0.2434, the minimum value is −0.41, and the mean value is 0. As the number of structure layers $\boldsymbol{a}$ is increased, the distinction between the kurtosis characteristics of the transient electromagnetic signal and the noise increases. However, as $\boldsymbol{a}$ increases, the scale of *SEs* will decrease, so that the denoising effect will be affected. Therefore, the number of structural layers $\boldsymbol{a}$ needs to be set reasonably.

In order to judge the extraction effect of abnormal signals at different SNR, *HML* indicators are constructed based on P^a_{g+} and P^a_{g-}, which is defined as:

$$HML = \left| V\left(P^a_{g+}\right) / V\left(P^a_{g-}\right) \right| \tag{13}$$

In Eq. (13), $V(P^a_{g+})$ is the amplitude of the rising edge signal extracted under different $\boldsymbol{a}$, and $V(P^a_{g-})$ is the amplitude of the falling edge signal. The physical meaning of *HML* is the extraction effect of MCDPMF on transient electromagnetic signals under different $\boldsymbol{a}$. And the *HML* value is positively correlated with the extraction effect. This article comprehensively considers the performance of $\boldsymbol{a}$, the length of *SEs* and *HML* value under different SNR. The relationship curve is shown in Fig.4:

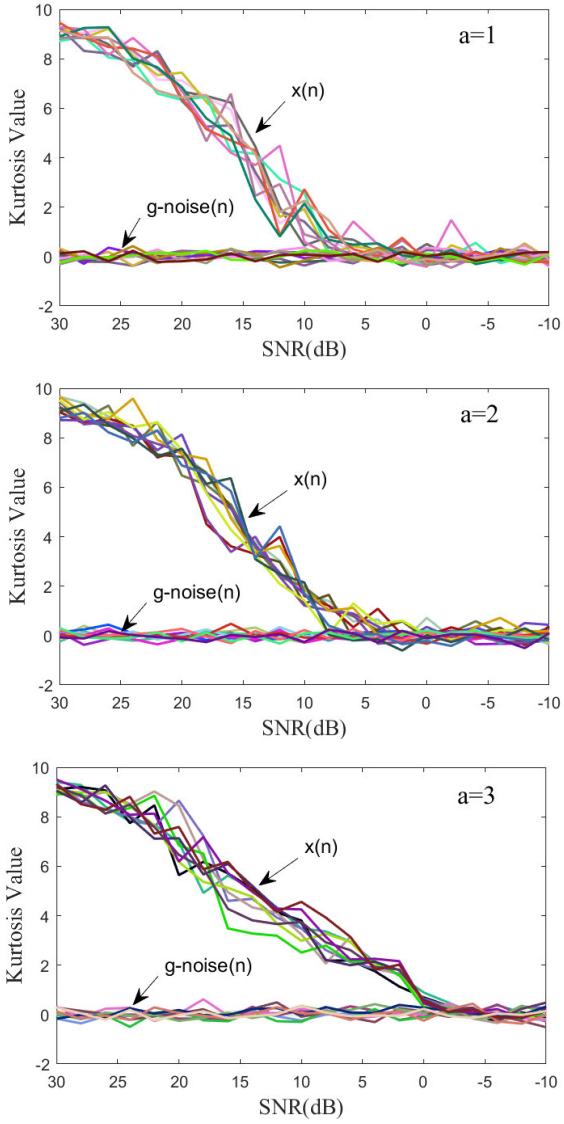

FIGURE 2. Changes of $k_x - SNR$ under different structural layers (a = 1-3).

In what follows, the relationship between $\boldsymbol{a}$ and *SEs* are explained in Fig.4. A high $\boldsymbol{a}$ corresponds to a small-scale *SEs*, which is limited to the conflict between the *SEs* scale in extracting detailed signal features and denoising effects. The choice of $\boldsymbol{a}$ can be adaptively optimized by combining *HML* indicators.

IV. SIMULATION TEST RESULTS

To further more explore the method of this paper, we used three SNR ratio's simulation signal (5dB, 0dB, and −5dB) to illustrate the effectiveness of the MCDPMF algorithm for extracting weak transient electromagnetic signals. The frequency range of the transient electromagnetic signal is 1-1000Hz, and the signal to be detected is simulated by

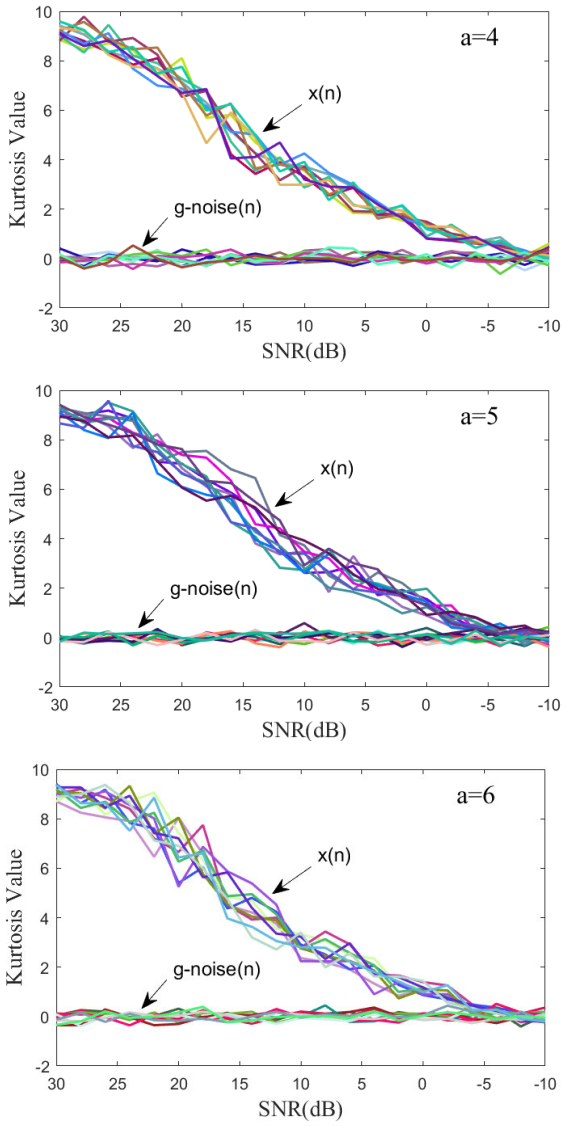

FIGURE 3. Changes of $k_x - SNR$ under different structural layers (a = 4-6).

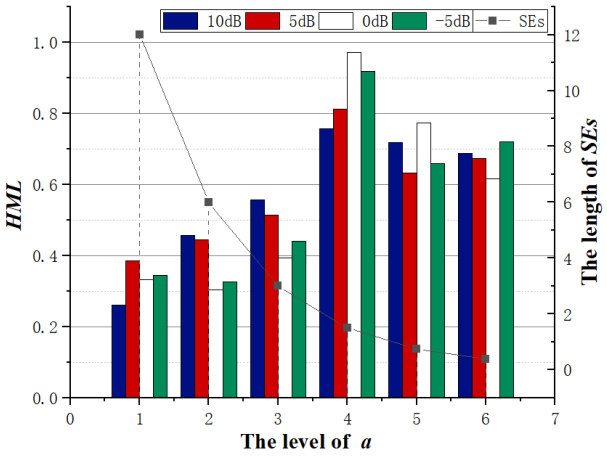

FIGURE 4. The relationship between *a*, *SEs* and *HML* indicators in the MCDPMF algorithm.

using a double exponential attenuated oscillation pulse:

$$y_1(t) = 1.2\sin(2\pi f_1 t) + 1.1\cos(2\pi f_2 t) \quad (14)$$

$$y_2(t) = 4e^{-100 \bmod (t,1/f_0)}\sin(400\pi t) \quad (15)$$

$$y(t) = y_1(t) + y_2(t) + \delta(t) \quad (16)$$

In Eq. (14), where $y_1(t)$ contains two interfering frequencies, and the f_1 and f_2 are 30 Hz and 40 Hz. In Eq. (15), $y_2(t)$ is an exponentially decaying oscillation signal with a frequency of 16 Hz, which is used to simulate weak transient electromagnetic signals. In Eq. (16), $\delta(t)$ is the added mixed noise, which includes the wide-spectrum white Gaussian noise, which is used to simulate the background thermal noise and random background environmental noise of the test system, as well as the periodic narrowband interference noise of analog broadcasting and communication. The simulated signal is shown in Fig.5, and it can be seen that the transient electromagnetic signal is overwhelmed by interference frequencies and noise signals, and the original signal cannot be distinguished in the time domain.

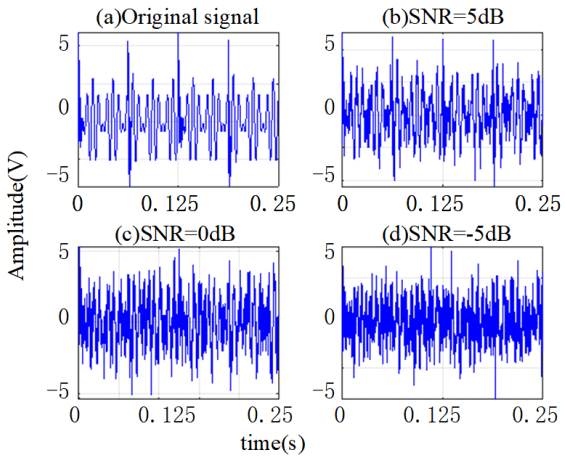

FIGURE 5. Simulation of transient electromagnetic weak signal, (a) Noiseless original signal (b) SNR = 5dB (c) SNR = 0dB (d) SNR = −5dB.

The spectrum and envelope spectrum analysis results of the transient electromagnetic signal with SNR of −5dB are shown in Fig.6. Due to the influence of strong noise and interference, the low-frequency electromagnetic signal cannot be extracted, and only the frequency of the interfering signal can be seen. Therefore, it is challenging to extract transient electromagnetic signals under strong noise background using spectrum and envelope spectrum analysis.

The MCDPMF algorithm proposed in this paper extracts weak signals $y(t)$ under the three SNR conditions which mentioned in Fig.5. In MCDPMF, the layers of multi-scale structure $\boldsymbol{a}$ has a great influence on the performance of electromagnetic transient signal detection in strong noise environment. In this chapter, we will further discuss the effect of transient electromagnetic signal extraction and pulse detection results under different SNR in the test results, and

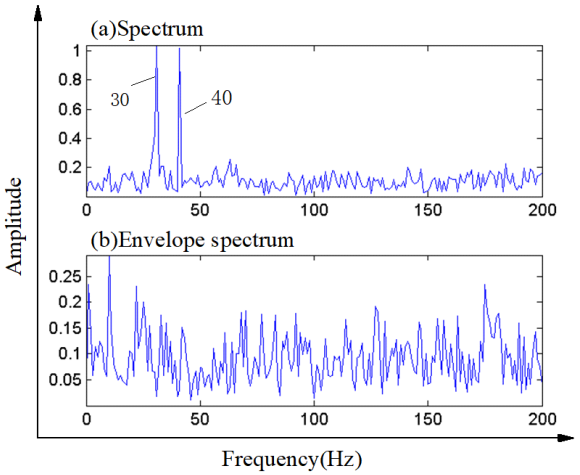

FIGURE 6. Spectrum and envelope spectrum analysis of $y(t)$ under -5dB.

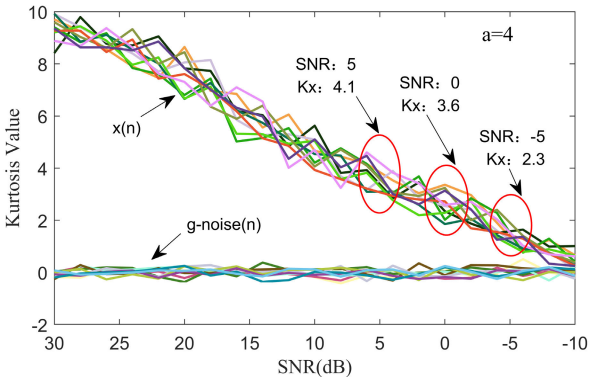

FIGURE 7. The change of $k_x - SNR$ in simulation results when a = 4. (SNR = 5dB, 0dB and -5dB).

combined with the adaptive selection of structural layers $\boldsymbol{a}$ and $k_x - SNR$. The calculation results of HML value of simulation results under multi-structure layers are listed in Table 1:

TABLE 1. HML value of simulation results (SNR = 5dB, 0dB, -5dB) under the multi-structure layers a of the MCDPMF.

HML value / SNR / a	5dB	0dB	-5dB
1	0.386	0.293	0.215
2	0.446	0.365	0.325
3	0.618	0.534	0.439
4	0.832	0.762	0.792
5	0.773	0.633	0.593
6	0.673	0.616	0.572

As can be seen from Table 1, the MCDPMF has the best HML value when a = 4, which means that the algorithm proposed in this paper shows good performance in transient signal detection in different SNR situations. At the same time, the results in Table 1 verify the effectiveness of the structural layer selection method proposed in Section 2.

Taking the test results of the structural layer of MCDPMF is four (a = 4), Fig.7 shows the change of characteristic coefficient of simulation results (SNR = 5dB, 0dB and -5dB), and the $k_x - SNR$ values under three different SNR are marked in the Fig.7.

As can be seen from Fig.7, we can find that MCDPMF has good discrimination under three SNR conditions, which further proves the effectiveness of the method proposed in this paper in extracting electromagnetic transient signals in low SNR and strong interference electromagnetic environment. Fig.8 respectively show the signal extraction effect after filtering.

Analysis of Fig.8 shows that when the weak transient electromagnetic signal is under 5dB, 0dB, and -5dB working conditions, through the MCDPMF, the signal is firstly filtered in the background of strong noise, and the polarity of the weak signal is judged by accurately extracting the pulse features of the rising and falling edge of the signal, the results are shown in Fig.8(b) respectively; Secondly, compared with Fig.8(a), the result as shown in Fig.8(c), we can get that the weak signal extraction is realized in a low SNR environment, while the added interference frequency (f_1, f_2) and mixed noise $\delta(t)$ are successfully suppressed. Synthesize the above discussion, the results show that MCDPMF can effectively extract weak transient electromagnetic signals in a strong noise environment.

V. EXPERIMENT AND DISCUSSION

An experimental was conducted to evaluate whether MCDPMF could extract and recognize transient signal in strong noise electromagnetic environment. During the experiment, based on the NI PXIE-5162 acquisition device and the analog radiation source device, the 80Hz transient discharge signal was injected into the power cable. The current caliper (ROHDE&SCHWARZ EZ-17) conjunction with the 30dB preamplifier (LANGER PA303N), was used to collect the transient electromagnetic signal at the sampling frequency of 3GHz. This paper uses a set of data of 0.1 s, and the data's time domain and frequency domain graphs are shown in Fig.9. The transient electromagnetic signal is difficult to detect because of its short duration, strong noise, and complex frequency components. Fig.9(a) shows that the time domain signal is submerged in the background noises. In addition, it is difficult to directly obtain the frequency component of the target transient signal in the frequency domain, as shown in Fig.9(b). The MCDPMF algorithm proposed in this paper is used to suppress the noise and extract the pulse component of the measured transient signal.

The extraction results of transient signals by the MCDPMF algorithm under different structural layers ($\boldsymbol{a}$ = 1-6) as shown in Fig.10. Combined with Fig.10, *HML* values used to evaluate the extraction effect of transient signals under different $\boldsymbol{a}$, the results as listed in Table 2. It can be seen that when $\boldsymbol{a} = 4$, the *HML* value is 0.68828, which is the best transient signal extraction effect.

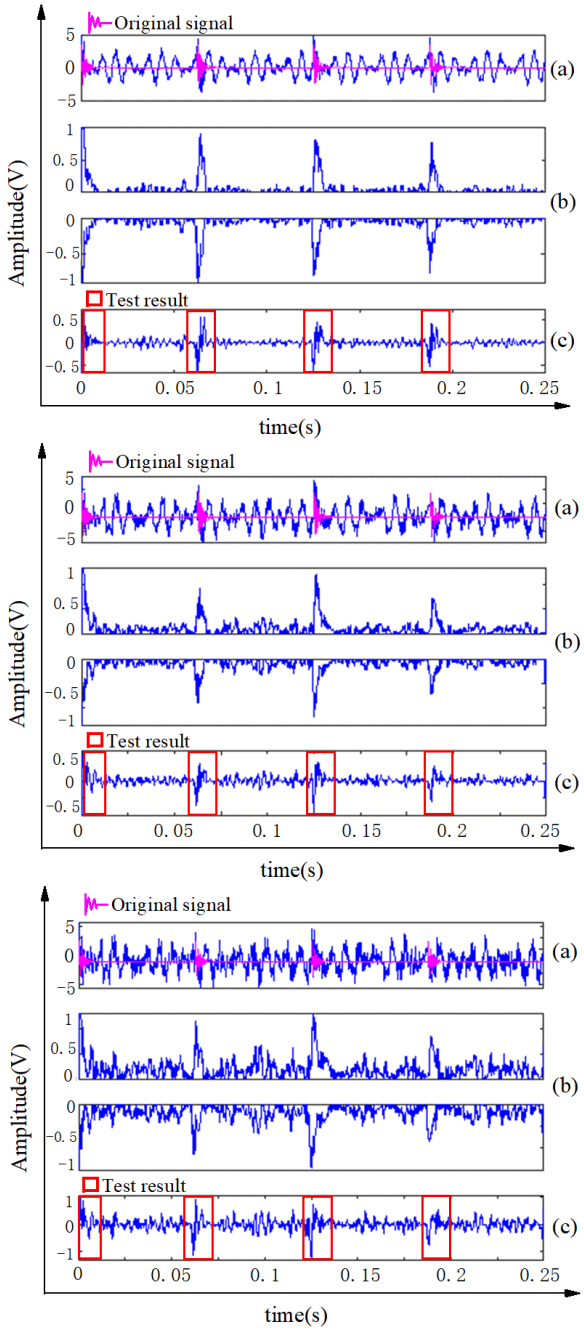

FIGURE 8. SNR = 5dB, SNR = 0dB, SNR = −5dB, transient electromagnetic signal $y(t)$ extraction effect. (a) Original signal with interference frequency and mixed noise under three different SNR working station(The three (a)'s represent: SNR = 5dB, 0dB, −5dB). (b) The polarity of the weak signal, including ascending and descending edge of transient signal(The three (b)'s represent: SNR = 5dB, 0dB, −5dB). (c) The weak signal extraction result by MCDPMF(The three (c)'s represent: SNR = 5dB, 0dB, −5dB).

TABLE 2. The HML value of MCDPMF under a = 1-6.

Figure number	(a)	(b)	(c)	(d)	(e)	(f)
a	1	2	3	4	5	6
HML value	0.0494	0.2001	0.6236	0.68828	0.5439	0.3368

The filtering and extraction effect of experimental data through the MCDPMF algorithm as shown in Fig.11.

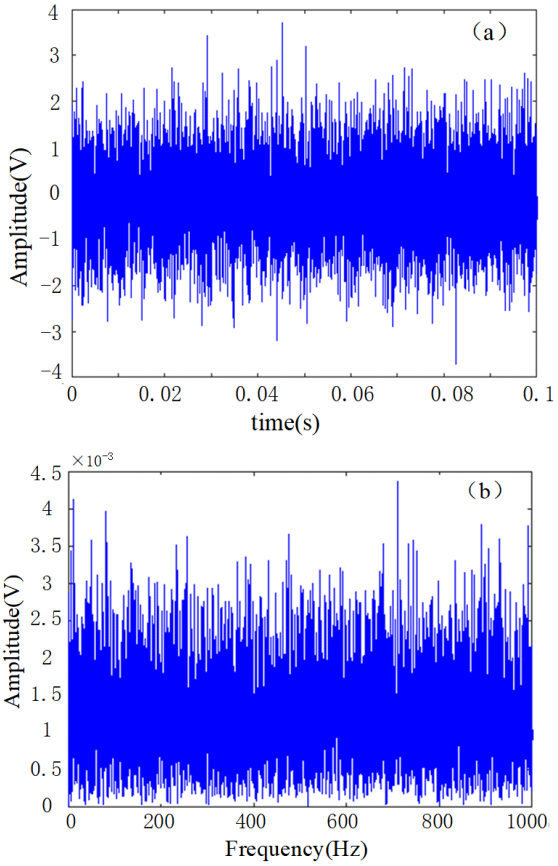

FIGURE 9. The experimental data. (a) Time-domain diagram (b) FFT spectrum.

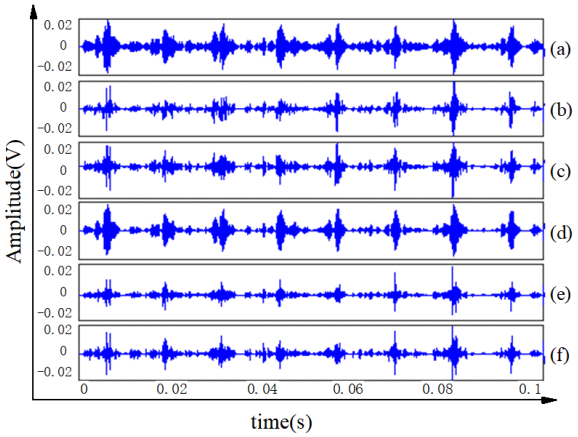

FIGURE 10. Extraction effect of the transient signal by MCDPMF under different structural layers (a = 1-6). (a) a = 1 (b) a = 2 (c) a = 3 (d) a = 4 (e) a = 5 (f) a = 6.

Fig.11(a) and (b) show the positive and negative pulse waveform of the experimental data signal, that is, the polarity (the rising and falling edge) of the signal. Fig.11(c) shows the extraction effect of the transient electromagnetic signals in the time domain. Combined with the effect of signal reconstruction and polarity characteristics, the signal's position information can also be obtained. The results of the spectrum analysis of the filtered signal are shown in Fig.11(d).

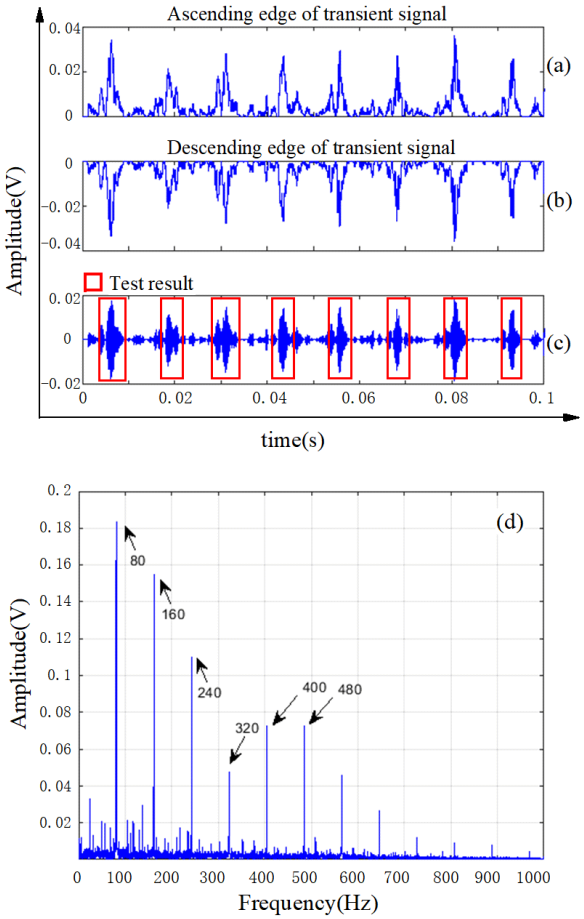

FIGURE 11. Transient signal extraction results based on MCDPMF (a) positive pulse (b) negative pulse (c) signal extraction result in time domain (d) FFT spectrum analysis.

Meanwhile, the frequency information of the transient signal ($f = 80$Hz) and its harmonic signal ($2f$, $3f$, $4f$) can be presented. The experimental results show that the transient signal extracted by MCDPMF has apparent resolution and a good suppression effect on interference and strong noise.

To further verify the effectiveness and general applicability of the proposed method, the transient weak signal extraction experiment is carried out with AVG, EMD, MG, OCCO, and MCDPMF; the experimental data is the same as above. The test results are shown in Fig.12.

The statistical domain's dimensionless features (*Kurtosis*, *Skewness*, *PeakFacter*, and *ImpulseFacter*) were used to compare the extraction effects. The *Kurtosis* represented the degree of steepness and slowness of the extracted signal, in other words, the magnitude of the peak value. *Skewness* represents the skew of the extracted transient pulse signal structure, that is the accuracy of structure extraction. *PeakFacter* and *ImpulseFacter* are used to detect whether the signal has a transient pulse. The extraction results of the five methods corresponding to the calculation results of the above four dimensionless features are shown in Table 3.

According to the analysis of the results listed in Table 3, the MCDPMF proposed in this article is significantly better than

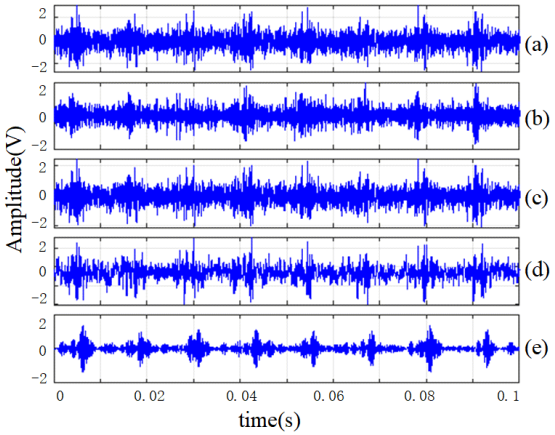

FIGURE 12. The effect of five methods for extracting transient signal. (a) AVG (b) EMD (c) MG (d) OCCO (e) MCDPMF.

the other four methods in *Kurtosis*, *Skewness*, *PeakFacter*, and *ImpulseFacter* indicators. The results prove that the algorithm proposed in this paper is the most accurate method in extracting weak transient electromagnetic signals, followed by EMD, OCCO, AVG, and MG.

TABLE 3. Four indicators calculation results.

Methods	Kurtosis	Skewness	PeakFacter	ImpulseFacter
AVG	4.363	0.171	8.916	11.603
EMD	4.462	0.150	9.188	12.18
MG	4.292	0.165	9.038	11.786
OCCO	4.461	-0.319	6.395	8.053
This paper	8.992	−0.0009	9.227	13.176

VI. CONCLUSION

The focus of this paper is to solve the problems of unknown structure and poor recognition effect of transient signal in low SNR and strong noise electromagnetic environment, and proposed a multi-scale combined difference product morphological filtering method (MCDPMF) based on improved basic morphological operators. Through the adaptive optimization of structural layers $\boldsymbol{a}$ by characteristic parameters and combined with multi-origin and scalable *SEs*, MCDPMF is constructed to suppress noise interference and extract transient weak signals. The simulation and experimental analysis results show that the proposed method is effective, it can give consideration to signal feature retention and noise suppression, and has a good capability of transient electromagnetic weak signal extraction. Compared with other filtering methods, the superiority of MCDPMF is verified. The method proposed in this article can be regarded as a problem of extracting weak periodic transient signals from measurement signals with strong background noise. Therefore, it can be applied to mechanical bearing fault diagnosis, late weak signal analysis of magnetotelluric, weak vibration signal extraction, and other fields.

REFERENCES

[1] S. Weiss, J. Matthews, and B. Jackson, "Weak transient signal detection via a polynomial eigenvalue decomposition," *Isaac Newton Inst., Future Math. Challenges Electromagn. Environ.*, pp. 1–18, Jul. 2021.
[2] J. Zhao, Z. Chen, X. Zhong, H. Che, and Y. Yu, "An enhanced transient extraction transform algorithm and its application in fault diagnosis," in *Proc. 40th Chin. Control Conf. (CCC)*, Jul. 2021, pp. 4356–4360.
[3] Z. Wang, J. Zhou, W. Du, Y. Lei, and J. Wang, "Bearing fault diagnosis method based on adaptive maximum cyclostationarity blind deconvolution," *Mech. Syst. Signal Process.*, vol. 162, Jan. 2022, Art. no 108018.
[4] Z. Wang, N. Yang, N. Li, W. Du, and J. Wang, "A new fault diagnosis method based on adaptive spectrum mode extraction," *Struct. Health Monitor.*, vol. 20, no. 6, pp. 3354–3370, Nov. 2021.
[5] Y. Li, X. Liang, and M. J. Zuo, "Diagonal slice spectrum assisted optimal scale morphological filter for rolling element bearing fault diagnosis," *Mech. Syst. Signal Process.*, vol. 85, pp. 146–161, Feb. 2017.
[6] H. Wang and W. Du, "Fast spectral correlation based on sparse representation self-learning dictionary and its application in fault diagnosis of rotating machinery," *Complexity*, vol. 2020, pp. 1–14, Aug. 2020.
[7] W. Li, Z. JiaQi, L. Yan, and P. ShuSheng, "Detection of radiometer radio frequency interference with power-law detector," in *Proc. Int. Appl. Comput. Electromagn. Soc. Symp.*, Aug. 2017, pp. 1–2.
[8] S. Govindarajan, M. Natarajan, J. A. Ardila-Rey, and S. Venkatraman, "Partial discharge location identification using permutation entropy based instantaneous energy features," *IEEE Trans. Instrum. Meas.*, vol. 70, pp. 1–12, 2021.
[9] R. B. Randall, "A history of cepstrum analysis and its application to mechanical problems," *Mech. Syst. Signal Process.*, vol. 97, pp. 3–19, Dec. 2017.
[10] A. Susanto, C.-H. Liu, K. Yamada, Y.-R. Hwang, R. Tanaka, and K. Sekiya, "Application of Hilbert–Huang transform for vibration signal analysis in end-milling," *Precis. Eng.*, vol. 53, pp. 263–277, Jul. 2018.
[11] A. Susanto, B. Artono, S. Khonjun, and R. Mahmud, "Denoising of disturbed signal using reconstruction technique of emd for railway bearing condition monitoring," *Int. J. Comput. Sci. Issues*, vol. 17, no. 5, pp. 15–22, Sep. 2020.
[12] D. Zhang, W. Ding, B. Zhang, C. Liu, J. Han, and D. Doermann, "Learning modulation filter networks for weak signal detection in noise," *Pattern Recognit.*, vol. 109, Jan. 2021, Art. no. 107590.
[13] Z. Wang, X. He, B. Yang, and N. Li, "Subdomain adaptation transfer learning network for fault diagnosis of roller bearings," *IEEE Trans. Ind. Electron.*, early access, Sep. 3, 2021, doi: 10.1109/TIE.2021.3108726.
[14] Z. Wang, W. Zhao, W. Du, N. Li, and J. Wang, "Data-driven fault diagnosis method based on the conversion of erosion operation signals into images and convolutional neural network," *Process Saf. Environ. Protection*, vol. 149, pp. 591–601, May 2021.
[15] Q. H. Wu, Z. Lu, and T. Ji, *Protective Relaying of Power Systems Using Mathematical Morphology*, vol. 45, 1st ed. New York, NY, USA: Springer, 2009.
[16] L. Liu, Z. Jia, J. Yang, and N. K. Kasabov, "SAR image change detection based on mathematical morphology and the K-means clustering algorithm," *IEEE Access*, vol. 7, pp. 43970–43978, 2019.
[17] P. Maragos and R. W. Schafer, "Morphological filters—Part I: Their set-theoretic analysis and relations to linear shift-invariant filters," *IEEE Trans. Acoust., Speech, Signal Process.*, vol. ASSP-35, no. 8, pp. 1153–1169, Aug. 1987.
[18] Z.-J. Li, F.-B. Yang, Y.-B. Gao, L.-N. Ji, and P. Hu, "Fusion method for infrared and other-type images based on the multi-scale Gaussian filtering and morphological transform," *J. Infr. Millim. Waves*, vol. 39, no. 6, pp. 810–817, Dec. 2021.
[19] J. Yu, T. Hu, and H. Liu, "A new morphological filter for fault feature extraction of vibration signals," *IEEE Access*, vol. 7, pp. 53743–53753, 2019.
[20] A. Hu and L. Xiang, "Selection principle of mathematical morphological operators in vibration signal processing," *J. Vib. Control*, vol. 22, no. 14, pp. 3157–3168, 2016.
[21] L. Yu, W. Dai, S. Huang, and W. Jiang, "Sparse time–frequency representation for the transient signal based on low-rank and sparse decomposition," *J. Acoust.*, vol. 1, Aug. 2019.
[22] A. E. Yilmaz, J. M. Jin, and E. Michielssen, "Analysis of low-frequency electromagnetic transients by an extended time-domain adaptive integral method," *IEEE Trans. Adv. Packag.*, vol. 30, no. 2, pp. 301–312, May 2007.
[23] Y.-F. Li, M. Zuo, K. Feng, and Y.-J. Chen, "Detection of bearing faults using a novel adaptive morphological update lifting wavelet," *Chin. J. Mech. Eng.*, vol. 30, no. 6, pp. 1305–1313, Nov. 2017.
[24] S. Gautam and S. M. Brahma, "Guidelines for selection of an optimal structuring element for mathematical morphology based tools to detect power system disturbances," in *Proc. IEEE Power Energy Soc. Gen. Meeting*, Jun. 2012, pp. 1–6.
[25] R. Godse and S. Bhat, "Mathematical morphology-based feature-extraction technique for detection and classification of faults on power transmission line," *IEEE Access*, vol. 8, pp. 38459–38471, 2020.
[26] M. A. Barik, A. Gargoom, M. A. Mahmud, M. E. Haque, A. M. T. Oo, and H. Al-Khalidi, "Mathematical morphology-based fault detection technique for power distribution systems subjected to resonant grounding," in *Proc. IEEE Power Energy Soc. Gen. Meeting*, Jul. 2017, pp. 1–5.
[27] S. Dong, B. Tang, and F. Chen, "De-nosing method based on multiscale morphological filter optimized by particle swarm optimization algorithm," *Chongqing Daxue Xuebao(Ziran Kexue Ban)*, vol. 35, no. 7, pp. 7–12, Jul. 2012.
[28] Y. Li, X. Liang, and M. J. Zuo, "A new strategy of using a time-varying structure element for mathematical morphological filtering," *Measurement*, vol. 106, pp. 53–65, Aug. 2017.
[29] Y. Dong, M. Liao, X. Zhang, and F. Wang, "Faults diagnosis of rolling element bearings based on modified morphological method," *Mech. Syst. Signal Process.*, vol. 25, pp. 1276–1286, May 2011.
[30] Q. Chen, Z. Chen, W. Sun, G. Yang, A. Palazoglu, and Z. Ren, "A new structuring element for multi-scale morphology analysis and its application in rolling element bearing fault diagnosis," *J. Vib. Control*, vol. 21, no. 4, pp. 765–789, 2015.
[31] A. S. Raj and N. Murali, "Early classification of bearing faults using morphological operators and fuzzy inference," *IEEE Trans. Ind. Electron.*, vol. 60, no. 2, pp. 567–574, Feb. 2013.
[32] Y.-S. Oh, J. Han, G.-H. Gwon, D.-U. Kim, C.-H. Noh, C.-H. Kim, T. Funabashi, and T. Senjyu, "Detection of high-impedance fault in low-voltage DC distribution system via mathematical morphology," *J. Int. Council Electr. Eng.*, vol. 6, no. 1, pp. 194–201, Jan. 2016.
[33] Z. Lu, Q. Wu, and J. Fitch, "A morphological filter for estimation of power system harmonics," in *Proc. Int. Conf. Power Syst. Technol.*, Oct. 2006, pp. 1–5.
[34] W. Jiang, Z. Zheng, Y. Zhu, and Y. Li, "Demodulation for hydraulic pump fault signals based on local mean decomposition and improved adaptive multiscale morphology analysis," *Mech. Syst. Signal Process.*, vols. 58–59, pp. 179–205, Jun. 2015.
[35] Y. Zhang, D. Zhu, and Q. Zhu, "Fault feature extraction for rolling element bearings based on multi-scale morphological filter and frequency-weighted energy operator," *J. Vibroeng.*, vol. 20, no. 8, pp. 2892–2907, Dec. 2018.
[36] X. Zhang, Z. Luan, and X. Liu, "Fault diagnosis of rolling bearing based on kurtosis criterion VMD and modulo square threshold," *J. Eng.*, vol. 2019, no. 23, pp. 8685–8690, Dec. 2019.
[37] X. Yan, M. Jia, W. Zhang, and L. Zhu, "Fault diagnosis of rolling element bearing using a new optimal scale morphology analysis method," *ISA Trans.*, vol. 73, pp. 165–180, Feb. 2018.
[38] J. Wang, G. Xu, Q. Zhang, and L. Liang, "Application of improved morphological filter to the extraction of impulsive attenuation signals," *Mech. Syst. Signal Process.*, vol. 23, no. 1, pp. 236–245, Jan. 2009.
[39] J. L. Naredo, J. A. Gutierrez, F. A. Uribe, J. L. Guardado, and V. H. Ortiz, "Frequency domain methods for electromagnetic transient analysis," in *Proc. IEEE Power Eng. Soc. Gen. Meeting*, Jun. 2007, pp. 1–7.
[40] A. C. Thompson and A. C. Thompson, *Minkowski Geometry*. Cambridge, U.K.: Cambridge Univ. Press, 1996.

JIANSHENG BAI received the B.S. and M.S. degrees in information and communication engineering from the North University of China, Taiyuan, China, where he is currently pursuing the Ph.D. degree with the School of Information and Communication Engineering. His research interests include laser detection, electromagnetic situational awareness, and signal processing.

JINJIE YAO was born in Shanxi, China, in 1982. He received the Ph.D. degree in information and communication engineering from the North University of China, Taiyuan, China, in 2011.

Since 2011, he has been an Associate Professor with the School of Information and Communication Engineering. Presided over and participated in six national basic scientific research projects, one 086 Project, one Key Research and Development Plan Project of Shanxi Province, one General Assembly Laboratory Fund, more than 20 horizontal scientific research projects, four invention patents authorized by the first inventor, and software copyright seven items. His research interests include microwave and millimeter wave technology and electromagnetic detection technology. In 2016, he won one First Prize of Shanxi Provincial Defense Technology Industry Science and Technology Innovation Award, and one Second Prize of Shanxi Provincial Science and Technology Invention Award, in 2021.

ZHILIANG YANG received the B.E. degree in electronics and information engineering from the North China Institute of Technology, Taiyuan, China, in 2003, the M.S. degree in signal and information processing from the North University of China, Taiyuan, in 2007, and the Ph.D. degree in communication and information systems from the Beijing Institute of Technology, Beijing, China, in 2015. He is currently as a Lecturer with the North University of China. His research interests include wireless channel modeling, physical layer security, and channel coding.

YURONG GUO received the B.S. degree in measurement and control technology, and instrumentation from the College of Modern Science and Technology, Taiyuan University of Technology, China. She is currently pursuing the M.S. degree in information and communication engineering with the North University of China. Her research interests include feature extraction and algorithm of electromagnetic signals.

LIMING WANG received the Ph.D. degree in measuring and testing technologies, and instruments from the North University of China, Taiyuan, China, in 2005. He is currently a Professor with the Department of Information and Communication Engineering, North University of China. His research interests include electromagnetic detection technology and nondestructive testing.